The Cryosphere Discuss.,
https://doi.org/10.5194/tc-2017-39-AC2, 2017

The Cryosphere Discussions

Interactive comment on "Understanding the Mechanism of Arctic Amplification and Sea Ice Loss" *by* Kwang-Yul Kim et al.

Kwang-Yul Kim et al.

kwang56@snu.ac.kr

Received and published: 7 July 2017

Comment1(C1): The paper applies a sort of regression analysis to the wintertime (JF) sea ice loss in the Barents-Kara seas. The review of prior literature on Arctic amplification and sea ice loss is often confusing, including in the definition of key concepts such as Arctic amplification or albedo feedback.

Response1(R1): Reviewer #2's comments are difficult to address because of the lack of detail in the review. More specificity is needed so that we can address the concerns of the reviewer. Which parts of the manuscript are confusing in terms of Arctic amplification and sea ice loss? What about the definition of Arctic amplification and albedo feedback is confusing? Arctic amplification represents a rapid warming of the Arctic

temperature, the physical interpretation of which may vary from one group of scientists to another. Albedo feedback is a feedback produced by albedo change. In summer, sea ice reduction decreases surface albedo in the Arctic Ocean, thereby increasing the absorption of solar energy in the ocean. This is referred to as albedo feedback in the manuscript.

C2: Based on the explanations given in the manuscript, I cannot understand the authors' methodology sufficiently to judge its value. The manuscript lacks a critical appreciation of the method, e.g. a discussion of how much of the time series and trend is actually captured by the first 'mode' obtained in the analysis.

R2: The methodology was published 20 years ago and has been used in many papers. We cannot repeat the full discussion on the methodology every time a paper is submitted. That is why three key references on the methodology have been added. We tried to improve the method section by including more specific details. [P3 L18-23: ... its amplitude varies from one year to another according to the corresponding PC time series. CSEOF loading vectors are mutually orthogonal to each other in space and time and represent distinct physical processes. The principal component (PC) time series, $T_n(t)$ are uncorrelated with (and are often nearly independent of) each other. Thus, each loading vector depicts a temporal evolution of spatial patterns seen in a physical process (such as El Niño or seasonal cycle), and corresponding PC time series describes a long-term modulation of the amplitude of the physical process.] [P4 L14-15: A rigorous mathematical explanation of the regression analysis in CSEOF space can be found in Kim et al. (2015).]

We also added how much of the total variability is explained by the sea ice loss mode. As can be seen in Fig. R1, the trend of sea ice reduction is most conspicuous in the Barents-Kara Seas. Figure R1a is very similar to Fig. 1a in the manuscript. Figure R1b also shows that sea ice reduction in the Barents-Kara Seas (red-boxed area in Fig. R1a) is well explained by the sea ice loss mode (red curve).

We made the following change in the revised manuscript: [P4 L17-18: Aside from the winter seasonal cycle, the first CSEOF mode derived from the daily winter sea ice concentration data depicts sea ice loss and associated Arctic warming in the Barents and Kara Sea. This mode explains 24% of the total variability of the sea ice concentration in the Artic Ocean and is the focus of investigation in the present study.] [P4 L23-26. . . 37 years (Fig. 1h). The pattern of sea ice reduction (Fig. 1a) is nearly identical with the trend pattern of sea ice concentration in the Arctic Ocean (see Fig. S1 in the supplementary information). As can be seen in Fig. 1h, the sea ice reduction trend in the Barents and Kara Seas (boxed area in Fig. 1a) is faithfully captured by this mode.]

C3: My fundamental concern with the manuscript is that it uses correlations to establish causalities and feedbacks, with little regard to the physical and meteorological phenomena discussed. As an example, the feedback loop suggested as a key result of the paper begins with sea ice reduction which supposedly causes warming of 850 hPa temperatures. The alternative explanation that warm air advection contributes to sea ice loss is at least as plausible, but not even mentioned in the manuscript.

R3: As we discussed in the "method of analysis" section, the CSEOF technique writes the space-time data in the form

$$T(r,t) = \Sigma_n B_n(r,t) T_n(t), \qquad (1)$$

where $B_n(r,t)$ represents the deterministic (physical) evolution associated with the nth CSEOF mode and $T_n(t)$ is the corresponding stochastic amplitude time series. Unlike EOF loading vectors, each CSEOF loading vector is time dependent and depicts physical (deterministic) evolution. In order to obtain physically consistent loading vectors from different variables, we used regression analysis in CSEOF space, the procedure of which is delineated in the manuscript. After regression analysis in CSEOF space, the entire dataset can be written as

$$Data(r,t) = \Sigma_n \{B_n(r,t), Z_n(r,t), U_n(r,t), \cdots\} T_n(t), \qquad (2)$$

where the terms in curly braces represent loading vectors from different variables. They are consistent in a physical sense.

Our statements are not solely based on correlations. At the very outset, we stated clearly that we would make a quantitative estimate of individual processes involved in an accelerated loss of sea ice concentration (P1 L22, P2 L28, P2 L30). It is the set of loading vectors in (2) that we are concerned with. For example, Fig. R2 above shows the time-averaged patterns of $\{B_n(r,t), Z_n(r,t), U_n(r,t), \cdots\}$ for the first CSEOF mode (sea ice loss mode). It shows how each variable behaves in accordance with the sea ice reduction in the Barents-Kara Seas. Another example is Fig. R3 above, where daily variation of each variable averaged over the region of sea ice reduction (red box in Fig. R1a). Based on this figure, we can understand how physical variables respond to the sea ice reduction over the Barents-Kara Seas, and in what way two or more variables are physically related with each other. As can be seen in Fig. R3, several variables evolve in a very similar manner over the region of sea ice reduction. It also shows how much the winter mean of each variable changes due to sea ice reduction. We do not know how correlation analysis could be used to make the physical inferences similar to those found in the present study.

As the reviewer mentioned, there are other processes such as warm advection that may be important for Arctic amplification and sea ice reduction. As can be seen in Fig. R4, there is a net convergence of moisture transport and heat transport over a region of sea ice reduction, although the center of action is over the Greenland Sea. Thus, moisture and heat transport from lower latitudes apparently affects the variation of sea ice concentration. Figure R5 further shows that there is appreciable correlation between the variation of specific humidity and convergence of moisture transport (corr=0.62) and between the variation of lower tropospheric temperature and convergence of heat transport (corr=0.33). Thus, it seems that both the convergence of moisture transport and the convergence of heat transport are responsible for the variation of specific humidity and temperature in the lower troposphere. On the other hand, the convergence

of horizontal transport of moisture cannot explain one essential element of the specific humidity anomaly–the mean of the anomalous specific humidity. As can be seen in Figure R5a, the mean of moisture convergence is close to 0.6×10^{-6} g/kg/sec, which amounts to ~ 0.05 g/kg of moisture. This value explains only about 17% of the mean value of anomalous specific humidity (~ 0.3 g/kg); the remainder should derive from a vertical process.

Consider the following moisture conservation equation:

$$\frac{\partial q}{\partial t} = -\vec{u} \cdot \nabla q + S \doteq -\nabla \cdot (q\vec{u}) + S = -\nabla_h \cdot (q\vec{u}) - \frac{\partial (qw)}{\partial z} + S. \qquad (3)$$

According to Fig. R5, the convergence of the horizontal moisture transport is not so effective as the convergence of the vertical moisture transport in the equation above in terms of increasing the mean of specific humidity. A positive convergence is offset by a negative convergence and vice versa, resulting in a small net increase in the mean of specific humidity. As can be seen in Fig. R6, the anomalous evaporation due to sea ice reduction is positive throughout the winter and its magnitude is reasonable in comparison with the increase in specific humidity. The two time series in Fig. R6 are negatively correlated (except for the mean), indicating that increased (decreased) specific humidity due to positive (negative) convergence of moisture transport reduces (augments) evaporation from the surface of the ocean; this is a reasonable explanation according to the bulk formula.

Likewise, the variation of the thermal advection and the subsequent convergence of the heat flux are highly correlated with the variation of downward longwave radiation and the lower tropospheric (850 hPa) temperature (see Fig. R5b). On the other hand, the small mean value of the convergence of the horizontal heat flux cannot explain the significant nonzero mean of the anomalous downward longwave radiation or the anomalous lower tropospheric (850 hPa) temperature. Thus, we conclude that the vertical process should be invoked in order to account for the significant changes in the

means of the variables over the Barents-Kara Seas. We did not simply ignore the contributions of moisture transport and heat transport from lower latitudes. Rather, this is a serious issue and requires more detailed calculation and convincing demonstration, which we considered beyond the scope of the present paper. We, however, acknowledge that we restricted ourselves to processes acting in the Arctic, ignoring the forcing from lower latitudes. Based on this discussion we made the following changes: [P3 L4-5: It should be noted that our discussion is restricted to processes in the Arctic; forcing from lower latitudes can also be important in the process of Arctic amplification and sea ice reduction.]

C4: I further do not see any justification for fitting an exponential to the time series of sea ice loss in the Barents-Kara seas, and far less for using that fit to make a prediction on when this ocean area would remain ice-free in winter.

R4: As can be seen in Fig. 1h in the manuscript, the exponential fitting looks reasonable in describing the change in sea ice concentration in the Barents-Kara Seas. One can use a linear or quadratic fit to make a similar prediction (see Fig. R7). Predictions are predictions whether it is based on the exponential fitting or the fitting of a low order polynomial; uncertainty is inherent in a prediction. We added the predictions based on linear fit and quadratic fit as supplementary information for the benefit of the readers. The reason why we chose the exponential fit (not on the sea ice concentration but on the PC time series of the sea ice loss mode in Fig. 1g in the manuscript) is that it yields the least residual error. The residual error based on a quadratic fit is similar to that of the exponential fit whereas a linear fit yields the largest residual variance among the three. We included some of this discussion and Fig. R7 as supplementary information. We also modified the text as follows: [P1 L24: ... sea ice will completely disappear in the Barents and Kara Seas by as early as 2025, although a conservative linear fit delays it until 2065.] [P7 L31: We fitted an exponential curve to the amplitude time series of the sea ice loss mode (Fig. 1g); an exponential fitting is chosen, since it minimizes the residual error. Our calculation shows that sea ice in the sea-ice loss region (21°-

79.5°E × 75°-79.5°N) of the Barents and Kara Seas may completely melt by as early as 2025 (Fig. 1h) unless impeded by other naturally occurring variability. A quadratic fit results in a similar result (2030 instead of 2025). A linear fit, the most conservative of the three but with the largest residual error, predicts a complete disappearance of sea ice in this area by 2065 (see Fig. S4).] We also updated the sea ice concentration curve using the 2017 sea ice data (see new Fig. 1h).

C5: In conclusion, I regret to say that the manuscript fails to meet basic scientific standards.

R5: We have addressed all specific comments and are not sure what standards we have failed to meet. We would be happy to address those if they would be identified.

** The combined response file including a marked-up manuscript is attached.

Please also note the supplement to this comment:
https://www.the-cryosphere-discuss.net/tc-2017-39/tc-2017-39-AC2-supplement.pdf

Interactive comment on The Cryosphere Discuss., https://doi.org/10.5194/tc-2017-39, 2017.

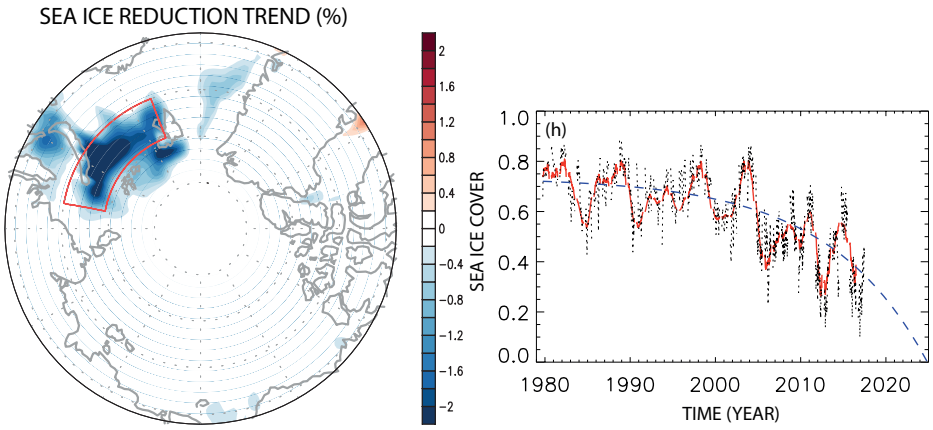

Fig. 1. The sea ice trend (% per year) in the Arctic Ocean (left panel) and the sea ice concentration in the red-boxed area of the Barents-Kara Seas (right panel).

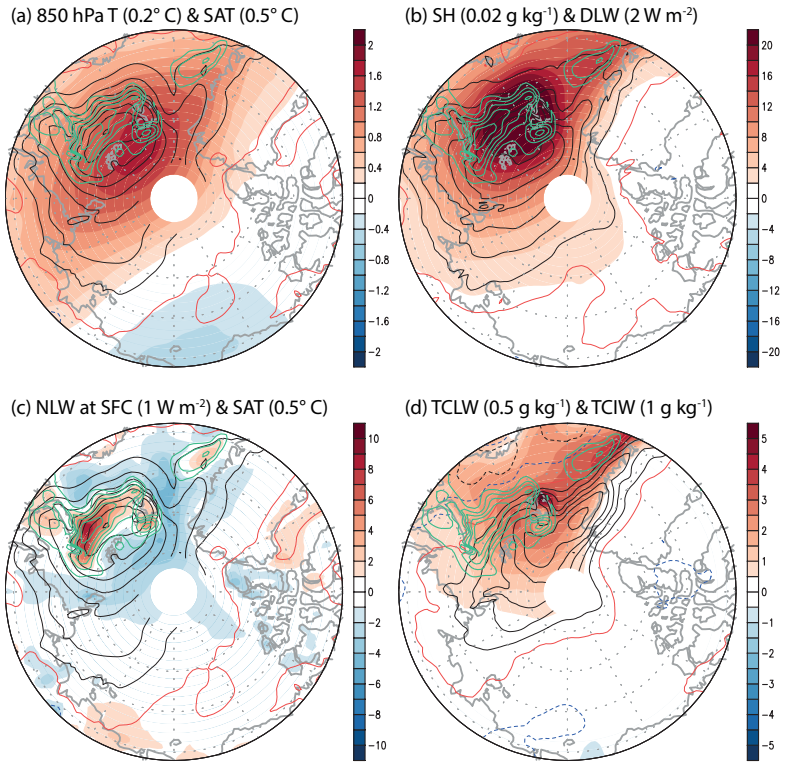

Fig. 2. The winter (DJF) averaged regressed patterns of several physical variables (reproduced from Fig. 4 in the manuscript). The caption of each panel shows the shading (contour) interval for the first (se

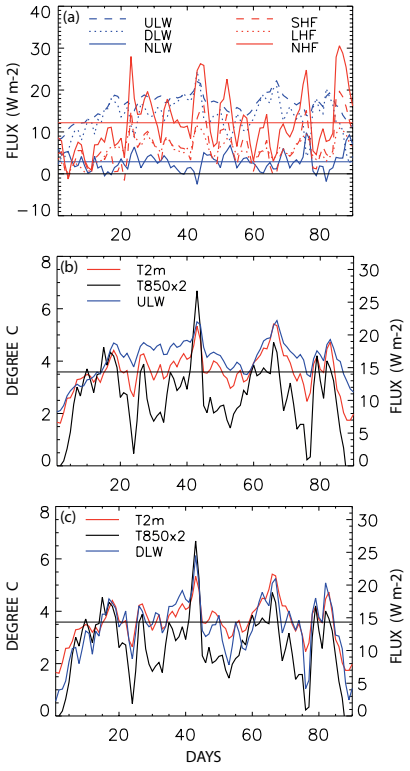

Fig. 3. The daily patterns of variability over the region of sea ice loss (21°-79.5°E × 75°-79.5°N) (reproduced from Figure 6 in the manuscript).

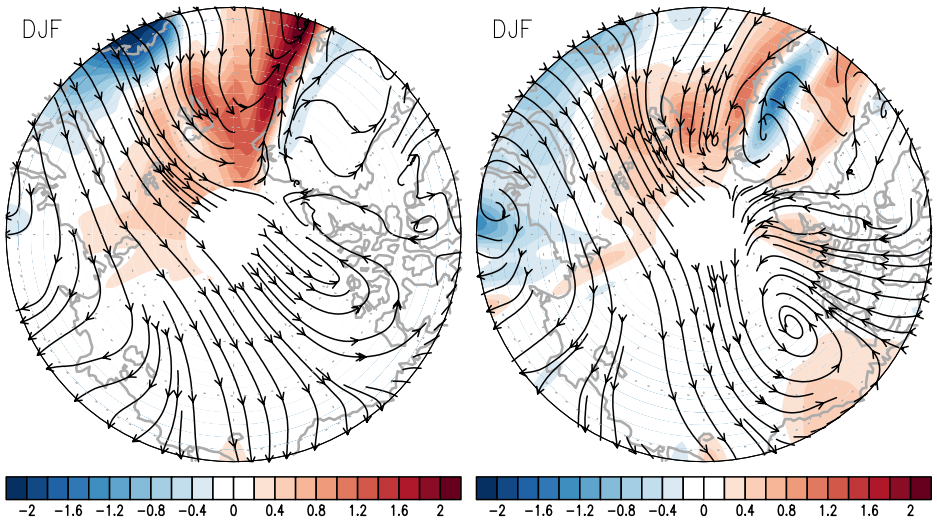

Fig. 4. Winter-averaged (left panel) moisture transport (streamline) and its convergence (shade) and (right panel) heat transport (streamline) and its convergence (shade) in the lower troposphere (1000-850 hP

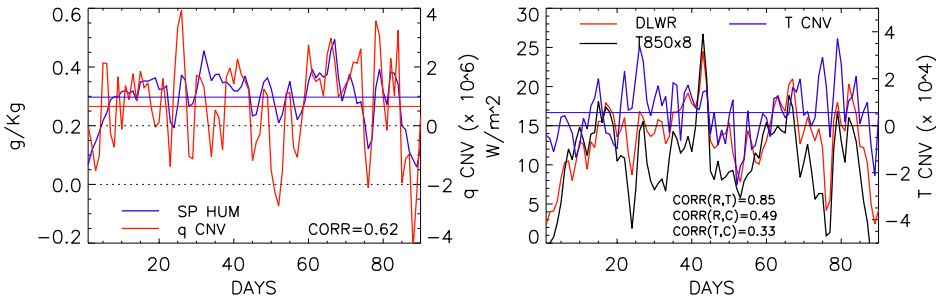

Fig. 5. The daily time series of anomalous specific humidity and anomalous moisture convergence averaged over the sea ice loss region (21°-79.5°E × 75°-79.5°N) in the Barents-Kara Seas. This particular time

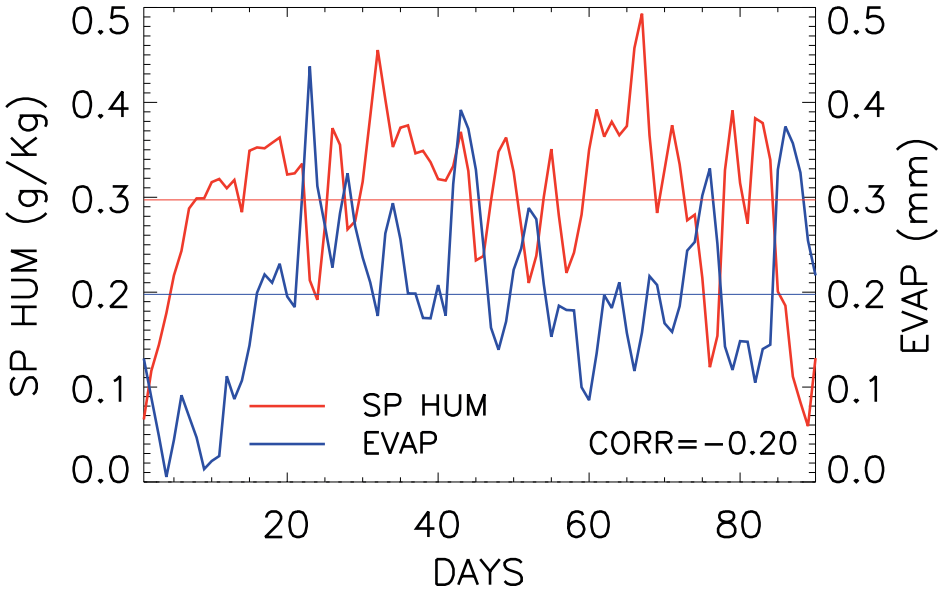

Fig. 6. The daily variation of specific humidity (red) and evaporation (blue) averaged over the region of sea ice reduction (21°-79.5°E × 75°-79.5°N) in the Barents-Kara Seas.

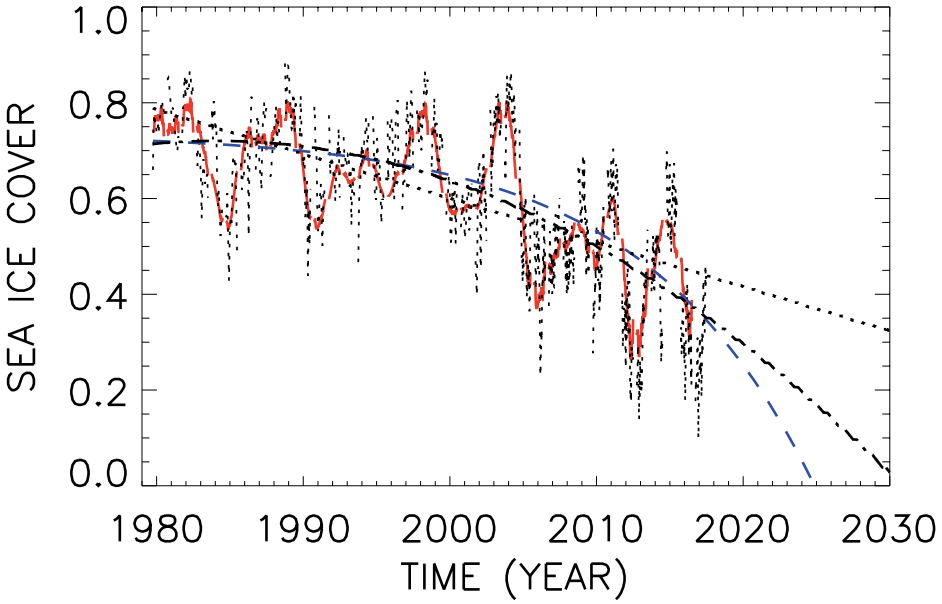

Fig. 7. Actual sea ice change in the sea-ice loss region (21°-79.5°E × 75°-79.5°N) of the Barents and Kara Seas (black dotted curve), sea ice change according to the sea ice loss mode (red curve), projections